Molecular Medicine

Adeno-associated Virus Serotype 8 (AAV8) Delivery of Recombinant A20 to Skeletal Muscle Reduces Pathological Activation of Nuclear Factor (NF)-κB in Muscle of *mdx* Mice

Rakshita A Charan,[1,2] Gabriela Niizawa,[1,2] Hiroyuki Nakai,[3] and Paula R Clemens[1,2]

[1]Neurology Service, Department of Veterans Affairs Medical Center, Pittsburgh, Pennsylvania, United States of America; [2]Department of Neurology, School of Medicine, University of Pittsburgh, Pennsylvania, United States of America; and [3]Department of Molecular and Medical Genetics, Oregon Health and Science University, Portland, Oregon, United States of America

Duchenne muscular dystrophy (DMD) is a genetic muscle disease caused by the absence of a functional dystrophin protein. Lack of dystrophin protein disrupts the dystrophin-glycoprotein complex causing muscle membrane instability and degeneration. One of the secondary manifestations resulting from lack of functional dystrophin in muscle tissue is an increased level of cytokines that recruit inflammatory cells, leading to chronic upregulation of the nuclear factor (NF)-κB. Negative regulators of the classical NF-κB pathway improve muscle health in the *mdx* mouse model for DMD. We have previously shown *in vitro* that a negative regulator of the NF-κB pathway, A20, plays a role in muscle regeneration. Here, we show that overexpression of A20 by using a muscle-specific promoter delivered with an adeno-associated virus serotype 8 (AAV8) vector to the *mdx* mouse decreases activation of the NF-κB pathway in skeletal muscle. Recombinant A20 expression resulted in a reduction in number of fibers with centrally placed nuclei and a reduction in the number of T cells infiltrating muscle transduced with the AAV8–A20 vector. Taken together, we conclude that overexpression of A20 in *mdx* skeletal muscle provides improved muscle health by reduction of chronic inflammation and muscle degeneration. These results suggest A20 is a potential therapeutic target to ameliorate symptoms of DMD.

Online address: http://www.molmed.org
doi: 10.2119/molmed.2012.00299

INTRODUCTION

Duchenne muscular dystrophy (DMD) is one of the most common muscle disorders, affecting about 1 in 3,500–6,000 males worldwide (1). It is caused by mutations in the dystrophin gene, resulting in the absence of or a dysfunctional dystrophin protein (2), and thus disruption of the dystrophin-glycoprotein complex (DGC) required for muscle membrane stability (3). Loss of the DGC causes increased tissue levels of several cytokines, such as tumor necrosis factor (TNF)-α, which recruits inflammation to the tissue (4,5) and activates the nuclear factor (NF)-κB signaling pathway (6,7). Chronic activation of the NF-κB pathway in muscle contributes to the onset and progression of DMD pathology in muscle by activating several downstream targets that affect muscle health (8–10). The NF-κB pathway plays a role in inducing the ubiquitin-proteasome pathway in muscle (11), causing increased protein degradation (12,13). Myogenic differentiation (MyoD) and myogenic factor-5 (Myf-5) are myogenic regulatory factors that play a role in normal murine muscle development and differentiation (14). MyoD expression was shown to be downregulated by the activation of the NF-κB pathway (15). Also, chronic activation of the NF-κB pathway in turn induces increased cellular infiltration of muscle, thus amplifying inflammation. Agents that prevent pathological activation of the NF-κB pathway have been shown to improve muscle health and decrease inflammation in muscle (16–18).

Several previous studies in *mdx* mice focused on inhibition of pathological NF-κB activation as a therapeutic target to ameliorate DMD symptoms. Inhibition of NF-κB activation in *mdx* mice promoted restoration of muscle membrane stability and regeneration capacity and led to a reduction in inflammation in muscle tissue (16,19). TNF-α–induced protein 3 (TNFAIP3), also known as A20, is a deubiquitinating enzyme that regulates NF-κB activation. A20 contains an N-terminal ovarian tumor (OTU) domain and seven C-terminal zinc-finger domains (20). TNF-α binds to its receptor and recruits the intracellular adaptor

Address correspondence to *Paula R Clemens, Department of Neurology, S520 Biomedical Science Tower, University of Pittsburgh, 203 Lothrop Street, Pittsburgh, PA 15213. Phone: 412-648-9762; Fax: 412-648-8081; E-mail: pclemens@pitt.edu.*
Submitted August 12, 2012; Accepted for publication November 5, 2012; Epub (www.molmed.org) ahead of print November 6, 2012.

The Feinstein Institute for Medical Research North Shore LIJ

protein receptor-interacting protein 1 (RIP1). A20 subsequently deubiquitinates RIP1 at lysine 63 and then reubiquitinates RIP1 at Lysine 48, marking it for degradation, thus inhibiting activation of the NF-κB signaling pathway (21). We have previously demonstrated that A20 plays a critical role in NF-κB pathway inhibition in skeletal muscle (22). Therefore, A20 has the potential to act as an intrinsic potent negative regulator of the NF-κB pathway, unlike many other therapeutic drugs currently being studied for amelioration of the pathway. Taken together, we hypothesized that delivery of recombinant A20 would offer therapeutic benefit for the treatment of dystrophic muscle in muscular dystrophy patients.

Recombinant adeno-associated virus (AAV) vectors are promising gene therapy delivery vehicles for a wide range of human diseases. There are different serotypes of AAV, and these show distinct tissue tropism and transduction efficiencies. AAV serotype 8 (AAV8) achieves a high efficiency of transduction of skeletal muscle and heart (23,24). AAV8 efficiently transduces both fast and slow skeletal muscle fibers with equal efficiency (25). Therefore, to explore the potential of A20 as a therapeutic target to ameliorate DMD symptoms in *mdx* mice, we used AAV8 to overexpress A20 in skeletal muscle. To restrict expression of A20 to skeletal muscle, we used the truncated muscle creatine kinase (tMCK) promoter (26). The tMCK promoter, which is about 720 base pair (bp) in length, was generated by ligating a triple tandem repeat of the MCK enhancer to its basal promoter, thus generating a strong, muscle-specific promoter (26) sufficiently small to be carried with the A20 cDNA by the AAV vector. Within muscle tissue, the tMCK promoter has preferential expression in fast-twitch fibers. The promoter, however, was shown to have weak expression in heart, diaphragm and liver (26). Here, we analyze the effects of A20 overexpression in skeletal muscle driven by a tMCK promoter by using an AAV8 vector.

MATERIALS AND METHODS

Mice and Reagents

C57BL/10ScSn-*Dmd*^{mdx}/J (*mdx*) mice were purchased from The Jackson Laboratory (Bar Harbor, ME, USA) and were housed at the University of Pittsburgh Animal Housing Facility and used under approval by the University of Pittsburgh Institutional Animal Care and Use Committee.

Antibodies used for Western blotting and immunohistochemical analyses were A20 (sc-22834), RelB (sc-28689), GAPDH (sc-25778), MyoD (sc-760) and Myf-5 (sc-302). The secondary antibody for Western blotting was goat anti-rabbit horseradish peroxidase (HRP) (sc-2030) (Santa Cruz Biotechnology, Santa Cruz, CA, USA). Antibodies for immune cells included those for CD4 T cells (16-0041-81) (eBiosciences, San Diego, CA, USA), CD8 T cells and secondary antibody, biotinylated goat anti-rat IgG (Pharmingen, San Jose, CA, USA). Monoclonal antibodies were used to detect myosin heavy chain (MHC, Fast and Slow) (Vector Laboratories, Burlingame, CA, USA). The monoclonal antibody to embryonic MHC (eMyHC) (F1.652), used to detect regenerating fibers, was obtained from the Developmental Studies Hybridoma Bank, developed by Helen Blau (University of Iowa, Department of Biological Sciences, Iowa City, IA, USA).

Virus Preparation and Injections

The recombinant AAV8-tMCK-A20 vector used in this study was constructed by using an A20 plasmid that was obtained from the BCCM/LMBP plasmid collection (LMBP 4801; Department of Biomedical Molecular Biology, Ghent University, Zwijnaarde, Belgium). The tMCK promoter DNA (26) and AAV-tMCK-GFP plasmid, used as a control, were obtained from Bing Wang (University of Pittsburgh, PA, USA). The tMCK-GFP expression cassette was carried by a double-stranded AAV (dsAAV) vector; however, the tMCK-A20 expression cassette was carried by a single-stranded AAV (ssAAV) vector because of its large size. For large-scale production of the virus, the three-plasmid cotransfection method was applied in AAV-293 cells, as described previously (42,43).

Neonatal *mdx* pups (2–3 d old; males and females) were given an intraperitoneal injection of 6.25×10^{10} vector genomes (vg) in a volume of about 30 μL. The numbers of mice injected are stated in Results. As a control, age-matched pups were given an intraperitoneal injection of 30 μL of either saline or AAV8-ISceI.AO7 vector, which is a modified version of AAV8-ISceI.AO3 (accession number-EU022316) (44). This vector does not express transgene products in mammalian cells.

Electrophoretic Mobility Shift Assay

Nuclear extracts were obtained from quadriceps and diaphragm muscle samples of vector- or saline-injected *mdx* mice by using NE-PER Nuclear and Cytoplasmic Extraction Reagent (ThermoFisher Scientific, Rockford, IL, USA). Protein concentrations of the extracts were measured by the BCA assay (ThermoFisher Scientific). To study NF-κB activity, the nuclear extracts were preincubated with 5× gel shift binding buffer (Promega, Madison, WI, USA) and nuclease-free distilled water. This step was followed by incubation with an α-^{32}P-deooxycytidine triphosphate (CTP)-labeled, double-stranded DNA probe containing the NF-κB binding domain (PerkinElmer, Waltham, MA, USA). The probe was added at a count per minute (cpm) of ~100,000/μL, to bring the final volume to 10 μL. The NF-κB probe was designed as described previously (45). Briefly, 15-bp annealing nucleotides were annealed to a 31-bp oligonucleotide template at the 3′ end of the template strand. The overhang was filled in with deoxyribonucleotide triphosphates (dNTPs) in conjunction with ^{32}P-dCTP by using Polymerase I, Large (Klenow) Fragment (Invitrogen; Life Technologies, Carlsbad, CA, USA). Labeled reactions were purified by using MicroSpin G50 columns (GE Healthcare, Piscataway, NJ, USA). Oligonucleotide sequences were as follows: NF-κB tem-

plate: 5′-CAGGG CTGGG GATTC CCCAT CTCCA CAGTT TCACT TC-3′; NF-κB annealing: 5′-GAAGT GAAAC TGTGG-3′ (Integrated DNA Technologies, Coralville, IA, USA). DNA protein complexes were separated on 6% polyacrylamide gels and resolved by electrophoresis in 1× Tris/borate/EDTA (TBE) buffer at 100 V for 1 h. The gel was then dried at 80°C for 1 h and autoradiographed at –80°C for 24–48 h.

Western Blot Analysis

Total lysates from quadriceps muscle and diaphragm tissues were obtained by using a T-PER Tissue Extraction Reagent (ThermoFisher Scientific). Lysates were run on a 10% sodium dodecyl sulfate–polyacrylamide gel electrophoresis (SDS-PAGE) gel for 1 h and transferred onto a Hybond nitrocellulose membrane at 100 V for 90 min. Membranes were blocked by using blocking buffer (1× phosphate-buffered saline [PBS] with 10% goat serum) for 1 h, followed by incubation with specific primary antibodies and HRP-conjugated secondary antibodies. The blot was then incubated with electrochemiluminescence reagents (GE Healthcare) and autoradiographed to visualize protein bands. Standard protein markers were run with proteins to determine protein size. All quantifications were performed by using MCID software (InterFocus Imaging, Cambridge, UK).

Muscle Tissue Processing

Hind limb muscles and diaphragms obtained from *mdx* mice were snap-frozen by using 2-methylbutane precooled on dry ice and stored at –80°C. For immunohistochemical analysis, tissue samples were sectioned at a thickness of 10 μm and transferred onto slides.

Immunohistochemical Analysis

Quadriceps and diaphragm sections were thawed at room temperature for 5 min and hydrated by using 1× PBS. The sections were then blocked by using blocking buffer (10% goat serum in 1× PBS) for 1 h and probed with specific primary and secondary antibodies diluted in DAKO antibody diluent (Invitrogen; Life Technologies). Sections were then washed and mounted by using Dapi-Fluoromount-G mounting medium in the dark. Sections that were incubated with anti-mouse antibodies were treated with an additional blocking step by using MOM Mouse IgG blocking reagent (Vector Laboratories) in 1× PBS for 1 h. The ratio of fibers with centrally placed nuclei in each group was quantified by counting fibers with centrally placed nuclei and the total number of fibers per field in a section of vector-injected quadriceps compared with saline-injected quadriceps, six to eight fields (~100–125 fibers per field) per section and two to three sections per mouse. The quantification of centrally nucleated, regenerating and necrotic fibers was carried out in a double-blinded manner by two independent researchers.

For CD4 and CD8 staining, we used a 3,3′-diaminobenzidine (DAB) staining protocol as described previously (46). Briefly, rehydrated sections were blocked in peroxidase blocking reagent (Invitrogen; Life Technologies) for 5 min and then incubated in blocking buffer (10% goat serum in PBS) for 1 h. The sections were then incubated with specific primary antibodies diluted in blocking buffer for 1.5 h. Sections were incubated for 1 h with secondary antibody diluted in DAKO antibody diluent. Sections were incubated with ABC Vectastain avidin-HRP detection solution (Vector Laboratories) for 30 min at room temperature and DAB peroxidase substrate solution (Vector Laboratories) for 4 min. Sections were counterstained with eosin to visualize muscle fibers. The number of infiltrating cells in each group was quantified by counting the total number of cells per field in a section of vector-injected quadriceps: eight fields (10× magnification) per section and two sections per mouse.

Statistical Analysis

All values are presented as means ± standard error of mean (SEM) from independent animals in each group. Significance was determined by using the two-tailed and unpaired Student t test. $p < 0.05$ was considered significant.

All supplementary materials are available online at www.molmed.org.

RESULTS

A20 Overexpression Driven by a Muscle-Specific Promoter Accomplished by AAV8 Vector–Mediated Gene Transfer

Knockdown of A20 caused chronic activation of NF-κB in *mdx* myotubes, indicating its role in pathway regulation (22). We hypothesized that overexpression of A20 in skeletal muscle would have a therapeutic benefit improving muscle health. To test this hypothesis, we produced an AAV8 vector to overexpress A20 driven by the tMCK promoter, for which expression is limited to muscle. The schematic of the plasmid used to generate AAV8-tMCK-A20 is shown in Figure 1. Each neonatal *mdx* pup was given an intraperitoneal injection of 6.25×10^{10} vg of AAV8-tMCK-A20 or saline. Treated and control mice were killed at 8 wks of age for collection of muscle tissues. We chose 8 wks as the time point for analysis, because the dystrophic symptoms in *mdx* mouse muscle reach a peak at 8–12 wks of age.

To confirm that AAV8 vector alone had no effect on dystrophic symptoms, a group of mice received AAV8-ISceI.AO7, an AAV8 vector that does not express the transgene product in mammalian cells, in the same manner. Comparison of NF-κB activation levels in quadriceps muscles of saline-treated and AAV8-ISceI.A07–treated mice, as determined by electrophoretic mobility shift assay (EMSA), revealed no significant difference in NF-κB activation (Supplementary Figure S1). Thus, we studied saline-treated mice as a control for further analysis. Also, as a control, to determine expression levels, age-matched neonatal *mdx* mice were treated with an intraperitoneal injection of ds-AAV8-tMCK-GFP,

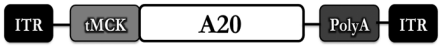

Figure 1. Schematic of the AAV-tMCK-A20 expression cassette. ITR, inverted terminal repeats.

and quadriceps muscles from these mice were analyzed for GFP expression. The dsAAV vector and the tMCK promoter were able to drive robust GFP expression in the heart and skeletal muscles, but not in the liver (Supplementary Figure S2) (26). We also compared levels of GFP expressed in various tissues by using the ubiquitous CMV promoter and observed lower GFP expression in skeletal muscles (tibialis anterior [TA] 0.39 ± 0.1, gastrocnemius 0.61 ± 0.2, quadriceps 0.57 ± 0.2; GFP protein levels normalized to GAPDH) compared with GFP driven by the tMCK promoter (TA 0.73 ± 0.3, gastrocnemius 0.77 ± 0.1, quadriceps 0.68 ± 0.1; GFP protein levels normalized to GAPDH; Supplementary Figure S2). These results were similar to those of an earlier study comparing various promoter-driven expression levels in differentiating C2C12 myoblasts (26).

Thus, we first assessed A20 protein levels in quadriceps muscles of the treated and control mice. We observed a 1.4-fold increase in A20 protein levels in quadriceps of *mdx* mice injected with AAV8-tMCK-A20 compared with saline-treated mice (Figure 2A). However, we did not observe any significant difference in A20 expression in diaphragms of *mdx* mice treated with A20 compared with saline (Figure 2B). The results in the diaphragm were expected because the tMCK promoter is known to have weak expression in this muscle (Supplementary Figure S2) (26).

Protein Levels of the RelB Subunit of NF-κB Alternate Signaling Pathway, and Myf-5 Muscle Differentiation Factor Increased on A20 Treatment

We previously showed that A20 is upregulated in regenerating fibers in skeletal muscle of *mdx* mice (22). Expression of RelB, a subunit of the alternate NF-κB

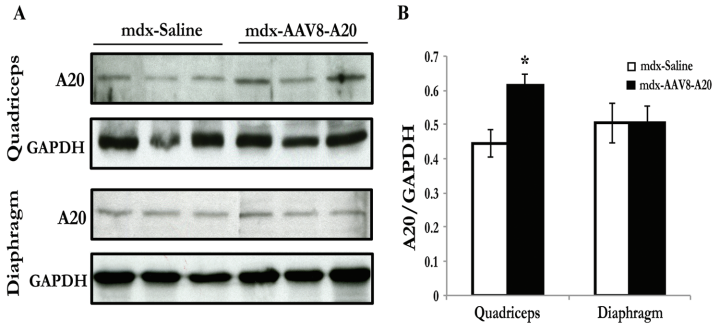

Figure 2. A20 protein levels in muscles of *mdx* mice treated with AAV8-tMCK-A20 compared with saline. (A) Total lysates from quadriceps and diaphragm muscles of 8-wk-old *mdx* mice treated with AAV8-tMCK-A20 or saline as neonates were analyzed for A20 protein levels by Western blotting. Results from three representative mice are shown. (B) Quantification of A20 protein levels normalized to GAPDH levels are shown. *$p < 0.05$. n = 9 for saline-treated *mdx* mice; n = 12 for AAV8-tMCK-A20–treated *mdx* mice.

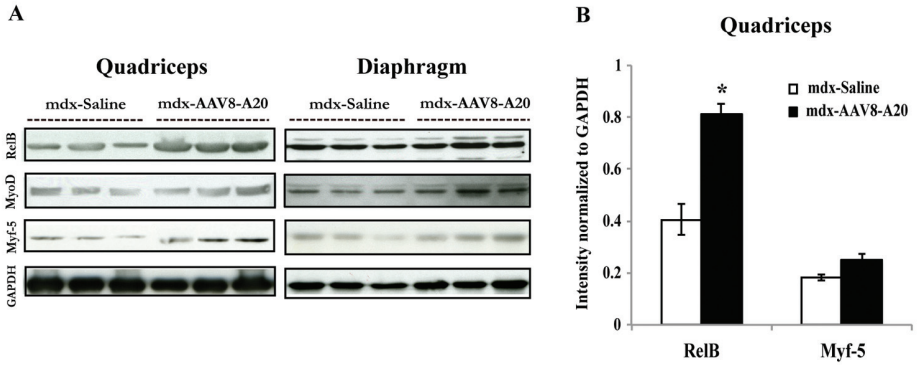

Figure 3. Protein levels of RelB and muscle differentiation factors MyoD and Myf-5. (A) Total lysates from quadriceps and diaphragm muscles of 8-wk-old *mdx* mice treated with AAV8-tMCK-A20 (AAV8-A20) or saline as neonates were analyzed for RelB, MyoD and Myf-5 protein levels by Western blotting. Results from three representative mice are shown. (B) Quantification of RelB and Myf-5 protein levels normalized to GAPDH levels are shown. *$p < 0.05$. n = 8 for saline-treated *mdx* mice; n = 8 for AAV8-tMCK-A20–treated *mdx* mice.

signaling pathway (27), was also upregulated in these fibers. Hence, we wanted to assess the effect of A20 overexpression on RelB protein levels. We observed a twofold increase in RelB protein levels in quadriceps of *mdx* mice treated with AAV8-tMCK-A20 compared with mice treated with saline (Figures 3A, B). We also analyzed protein levels of MyoD, and Myf-5, transcription factors required for differentiation of muscle. We observed a 1.3-fold increase in Myf-5 protein levels, but not MyoD levels, in quadriceps of AAV8-tMCK-A20–treated *mdx* mice compared with saline-treated *mdx* mice (Figures 3A, B). These levels were unchanged in the diaphragm of *mdx* mice treated with AAV8-tMCK-A20 compared with saline, as expected, since the tMCK promoter does not drive expression in diaphragm muscle (Figure 3A) (26).

A20 Overexpression Decreased Activation of the Classical NF-κB Pathway

A20 plays a critical role in negatively regulating the TNF-α–induced classical

NF-κB pathway activation in skeletal muscle–derived cells. Knockdown of A20 in *mdx* myotubes caused chronic activation of the NF-κB pathway (22). We assessed NF-κB pathway activity in quadriceps and diaphragm of control C57 mice and *mdx* mice treated with either AAV8-tMCK-A20 or saline. As expected, we see minimal activation of the NF-κB pathway both in the quadriceps and diaphragm muscles of C57 mice (Figure 4A). We observed a significant reduction in NF-κB pathway activation in mice treated with AAV8-tMCK-A20 compared with saline in quadriceps by EMSA (Figure 4A). In the diaphragm of AAV8-tMCK-A20–treated *mdx* mice, however, we did not see a significant a reduction in NF-κB activity (Figure 4B). This is an expected finding, since there was no increase in A20 expression in the diaphragm of AAV8-tMCK-A20–treated *mdx* mice and it is known that the tMCK promoter does not drive expression in the diaphragm muscle (26). Therefore, the subsequent analysis is limited to the limb muscle quadriceps.

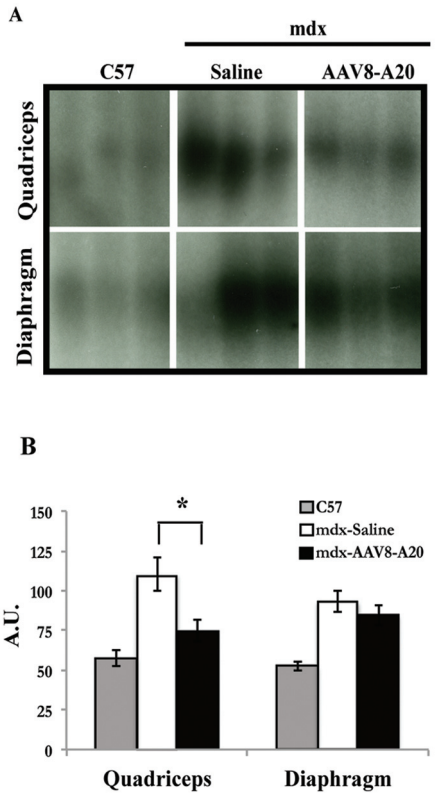

Figure 4. Electromobility shift assay of NF-κB activation in *mdx* quadriceps and diaphragm. (A) Nuclear extracts from quadriceps and diaphragm of C57 and *mdx* mice treated with AAV8-tMCK-A20 (AAV8-A20) or saline were assessed for NF-κB activity by using an EMSA. Results from three representative mice from each group are shown. (B) Quantification of NF-κB activation. Band intensities from each blot were measured and averaged for each group. *$p < 0.05$. n = 3 for C57 mice; n = 9 for saline-treated *mdx* mice; n = 12 for AAV8-tMCK-A20–treated *mdx* mice. A.U., arbitrary units.

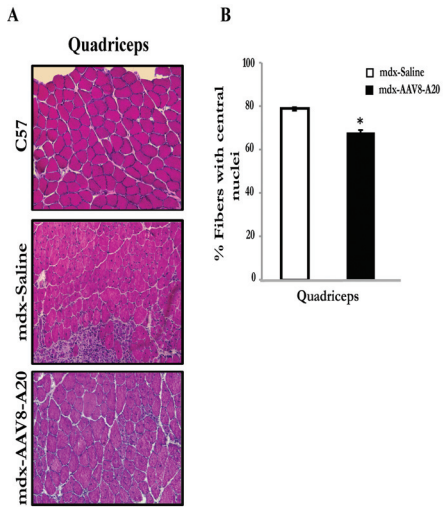

Figure 5. Histological analysis of quadriceps muscle of AAV8-tMCK-A20– and saline-injected *mdx* mice. (A) Muscle sections of quadriceps from C57 mice and *mdx* mice treated with AAV8-tMCK-A20 or saline were stained using hematoxylin and eosin to visualize muscle morphology and location of nuclei. (B) Quantification of number of fibers with centrally placed nuclei in quadriceps of saline- or AAV8-tMCK-A20–treated *mdx* mice. *$p < 0.05$. n = 9 for saline-treated *mdx* mice; n = 12 for AAV8-tMCK-A20–treated *mdx* mice. Scale bar = 150 μm.

Overexpression of A20 Causes a Decrease in the Number of Fibers with Centrally Placed Nuclei in *mdx* Quadriceps Muscle

One effect of the chronic activation of the NF-κB pathway in dystrophin-deficient muscle is an increase in protein degradation and ultimate muscle fiber atrophy (12,28), which leads to the activation of satellite cells to facilitate muscle regeneration (29). Thus, myofibers undergo repeated cycles of degeneration and regeneration, which prevents full muscle fiber maturation and is reflected in an increased percentage of fibers with centrally placed nuclei. We calculated the ratio of fibers with centrally placed nuclei to the total number of fibers to obtain a percentage of fibers with centrally placed nuclei. We observed a significant decrease in the percentage of fibers with centrally placed nuclei in quadriceps of A20-treated mice compared with saline-treated mice (Figures 5A, B).

A20 Overexpression Decreases Regeneration, but Has No Effect on Necrosis in *mdx* Quadriceps Muscle

Because we observed a decrease in the number of fibers with centrally placed nuclei, which reflects a reduction in the amount of muscle degeneration and regeneration, we analyzed markers for necrotic fibers (IgG uptake) and regenerating fibers (embryonic myosin heavy chain) in quadriceps tissue sections. We observed a decrease in the percentage of regenerating fibers in the quadriceps of AAV8-tMCK-A20–treated mice compared with saline-treated mice (Figures 6A, B). However, the decrease in the percentage of necrotic fibers in quadriceps muscle observed in AAV8-tMCK-A20–treated mice was not significant (Figure 6C).

Decrease in Infiltrating Inflammatory T Cells in Quadriceps Muscle of *mdx* Mice Treated with AAV8-tMCK-A20

Chronic inflammation in dystrophic muscle is one of the factors leading to protein degradation and subsequent muscle atrophy. A pathological increase in NF-κB activation results in increased cytokine expression and infiltration of inflammatory T cells. Because overexpression of A20 caused a reduction in NF-κB

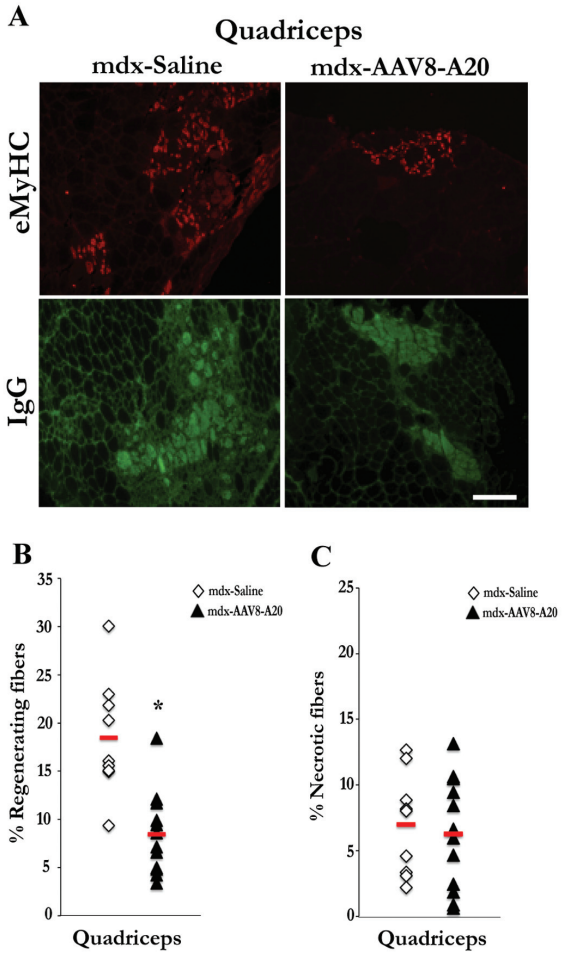

Figure 6. Analysis of regeneration and necrosis in quadriceps of *mdx* mice. (A) Muscle sections of quadriceps from *mdx* mice treated with AAV8-tMCK-A20 (AAV8-A20) or saline were labeled with embryonic myosin heavy chain (eMyHC) antibody (red) or IgG (green) to assess the number of regenerating fibers and necrotic fibers, respectively. Quantification of the percentage of regenerating (B) and necrotic (C) fibers is shown. n = 9 for saline-treated *mdx* mice; n = 12 for AAV8-tMCK-A20–treated *mdx* mice. Scale bar = 100 μm; $*p < 0.05$.

activation in muscle, we analyzed quadriceps muscles of AAV8-tMCK-A20–treated and saline-treated mice for the presence of CD4 and CD8 inflammatory T cells. In quadriceps from AAV8-tMCK-A20–treated mice, we observed a significant decrease in the number of CD4 T cells, but not CD8 T cells, compared with saline-treated mice (Figures 7A, B).

DISCUSSION

Chronic activation of the classical NF-κB signaling pathway in DMD muscle leads to many of the pathological symptoms in DMD (6,30), and it has been shown that inhibition of NF-κB activation ameliorates dystrophic muscle pathology (17,19). We show, for the first time, the role of A20 overexpression as a potential therapeutic target for DMD in *mdx* mice. We assessed the effect on skeletal muscle pathology in *mdx* mice of muscle-specific overexpression of A20. We found that increased protein expression of A20 led to a significant decrease in NF-κB pathway activation in quadriceps of *mdx* mice. We also observed an increase in protein levels of RelB, a subunit of the alternate pathway of NF-κB activation, and Myf-5, a muscle transcription factor required for differentiation. Moreover, we observed a decrease in the number of fibers with centrally placed nuclei and a decrease in markers of regeneration in the quadriceps of *mdx* mice. Lastly, we detected a reduction in the number of infiltrating inflammatory CD4 T cells in the AAV8-tMCK-A20–treated quadriceps. Taken together, we can conclude that A20 overexpression can reduce the activation of NF-κB and is thus an attractive candidate to further explore as a therapeutic target for the treatment of DMD.

Expression of A20 after systemic delivery with an AAV8 vector carrying the murine A20 cDNA driven by the muscle-specific tMCK promoter was increased 1.4-fold in quadriceps. One possible reason for this modest increase in A20 protein levels may have been due to delivery of an insufficient number of viral genomes. Also, levels of A20 may be affected by its expression by a single-stranded AAV (ssAAV) and not double-stranded AAV (dsAAV) vector. Our studies confirmed prior findings that the dsAAV vector and the tMCK promoter were able to drive robust GFP expression in the heart and skeletal muscles, but not in the liver (26). We confirmed, however, that the tMCK promoter provided transgene expression levels in skeletal muscle that was superior to the ubiquitous CMV promoter. Thus, even with the modest 1.4-fold increase of A20 expression, we provide proof-of-concept by the observation of a significant reduction in the activation of the NF-κB pathway in skeletal muscle. This result supports the hypothesis that overexpression of A20 would regulate the NF-κB pathway in muscle.

Interestingly, we also observed an increase in the expression levels of RelB, which reflects the NF-κB alternate pathway. We previously showed that RelB is overexpressed in regenerating fibers of dystrophic muscle and that A20 plays a role in muscle regeneration by inhibiting the classical but not the alternate pathway of NF-κB activation. Also, the alternate pathway of NF-κB activation was shown by others to be required for myo-

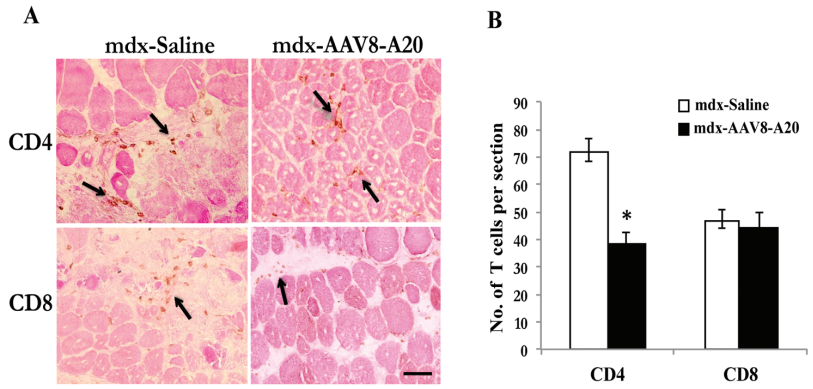

Figure 7. Analysis of infiltrating CD4 and CD8 T cells in quadriceps of *mdx* mice. (A) Muscle sections of quadriceps muscles from AAV8-tMCK-A20-treated (AAV8-A20) treated or saline-treated *mdx* mice were immunolabeled for CD4 and CD8 T cells. Sections were counterstained with eosin to visualize fibers. (B) Quantification of the number of CD4 and CD8 T cells per section of quadriceps muscles from AAV8-tMCK-A20– or saline-treated *mdx* mice. *$p < 0.05$. n = 9 for saline-treated *mdx* mice; n = 12 for AAV8-tMCK-A20–treated *mdx* mice. Scale bar = 20 μm.

genesis and maintenance of mature myofibers (31). Thus, we can speculate that overexpression of A20 inhibits the classical pathway of NF-κB activation, which leads to the upregulation of the alternate pathway, promoting muscle regeneration. We also observed an increase in Myf-5, but not MyoD, levels in quadriceps of AAV8-A20–treated mice. Myf-5 and MyoD play essential but redundant roles in muscle development (14), which might explain our findings of increased expression of Myf-5 but not MyoD. However, the dose-dependent effect of AAV8-A20 on the levels of these transcription factors remains to be evaluated.

Absence of dystrophin in skeletal muscle leads to loss of integrity of the muscle membrane, causing muscle fibers to undergo cycles of degeneration and regeneration (32,33). Because of this constant damage to muscle, myofibers become unstable, ultimately leading to protein degradation and muscle atrophy (32). We analyzed the effect of overexpression of recombinant A20 in quadriceps of AAV8-tMCK-A20–treated *mdx* mice on this cycle of damage and repair and observed a significant decrease in the number of fibers with centrally placed nuclei, a well-studied marker of continuous degeneration and regeneration. Earlier studies have also shown that reduced activation of the classical NF-κB pathway causes decreased regeneration and increased stability of muscle (17,34). Consistent with these studies, we also observed a decrease in the number of regenerating fibers in quadriceps of AAV8-A20–treated *mdx* mice. This result suggests a decrease in the damaging cycles of myofiber degeneration and regeneration and an overall improvement in muscle health and stability in the skeletal muscles.

The muscle pathology in DMD is thought to be caused by an imbalance between the amount of regeneration and the amount of necrosis in muscle tissue (32). One of the reasons muscle fibers degenerate is because of NF-κB–induced activation of transcription targets such as MuRF1 and atrogin-1 that mediate upregulation of the ubiquitin-proteasome pathway causing degradation of muscle fibers (28,35,36). We analyzed the effect of A20 overexpression on the number of necrotic fibers in skeletal muscle of treated *mdx* mice. Surprisingly, overexpression of A20 did not have any effect on necrosis in quadriceps muscle collected at 8 wks of age. We observed no change in the number of necrotic fibers in AAV8-tMCK-A20–treated compared with saline-treated *mdx* mice. Thus, although we observe a reduction in the markers for regeneration in quadriceps muscles, there is no change in degeneration in the muscles of the treated mice. One explanation for this could relate to the relatively low dose of the A20 transgene delivered to each mouse. Because the A20 transgene was delivered to neonates, its early expression during development could help to maintain the health and stability of muscle fibers by inhibiting activation of the NF-κB pathway. However, the relatively low A20 transgene expression may not have been sufficient to sustain its function to completely inhibit NF-κB activation leading to the transcription of its downstream targets, thus causing necrosis of muscle fibers. Future studies to determine a dose effect of the delivered transgene and the effect of mouse age at the time of gene transfer could aid in the further understanding of the dynamic relationship between necrosis and regeneration in diseased skeletal muscle.

Chronic activation of the NF-κB pathway in skeletal muscle leads to increased concentrations of cytokines and chemokines and the infiltration of inflammatory cells such as macrophages (37). Specifically, CD4 and CD8 T cells were shown to play a role in dystrophic pathology, and depletion of these cells led to improvement of histopathology in *mdx* mice (38). Because A20 causes reduction of the classical NF-κB pathway activation, we speculated that this reduction would decrease the amount of inflammation in muscle. We observed a reduction in the number of infiltrating CD4 T cells in the quadriceps of AAV8-tMCK-A20–treated *mdx* mice. We did not, however, observe any decrease in the number of CD8 T cells in these mice. Although, both CD4 and CD8 T cells are known to play a role in inflammation in *mdx* mice, CD4 T cells are more prevalent in *mdx* muscle (38). Furthermore, muscle biopsies from DMD patients showed a predominance of CD4 T cells compared with CD8 T cells (32,39). Also, CD4 T cells were found to colocalize with macro-

phages and degenerating muscle fibers, whereas CD8 T cells were scattered throughout muscle tissue (39). Hence, it was speculated that CD4 T cells, and not CD8 T cells, played a major role in causing cytotoxic muscle damage (39,40). A recent study showed that AAV vectors alone were capable of activating the alternate NF-κB pathway in HeLa cells (41). This was an interesting observation from a therapeutic point of view, since AAV-mediated transfer would be able to not only inhibit the classical pathway, reducing inflammation, but also promote activation of the alternate pathway, promoting improved muscle health.

CONCLUSION

Here we show that A20 is a potent negative regulator of the classical NF-κB pathway and plays a role in muscle regeneration by inhibition of this pathway in *mdx* mouse muscle. A20-mediated inhibition of the NF-κB pathway led to decreased dystrophic pathology and improved muscle health. Thus, AAV-mediated delivery of A20 should be explored further as a promising therapeutic target for DMD, and future studies need to be carried out to elucidate the exact mechanism and function of A20 in skeletal muscle.

ACKNOWLEDGMENTS

The authors thank Daniel Reay and Aditee Shinde for technical assistance and advice. We also thank Bing Wang, PhD, for provision of the AAV-tMCK-GFP plasmid. This work was supported by a VA Merit Review grant and University of Pittsburgh departmental funds and in part was supported by grant DK078388 to H.N.

The authors take full responsibility for the contents of this paper, which do not represent the views of the Department of Veterans Affairs or the U.S. Government.

DISCLOSURE

The authors declare that they have no competing interests as defined by *Molecular Medicine*, or other interests that might be perceived to influence the results and discussion reported in this paper.

REFERENCES

1. Emery AE. (1991) Population frequencies of inherited neuromuscular diseases: a world survey. *Neuromuscul. Disord.* 1:19–29.
2. Hoffman E, Brown R, Kunkel L. (1987). Dystrophin: the protein product of the Duchenne muscular dystrophy locus. *Cell*. 51:919–28.
3. Matsumura K, Ervasti JM, Ohlendieck K, Kahl SD, Campbell KP. (1992) Association of dystrophin-related protein with dystrophin-associated proteins in mdx mouse muscle. *Nature.* 360:588–91.
4. Pierno S, *et al.* (2007) Role of tumour necrosis factor alpha, but not of cyclo-oxygenase-2-derived eicosanoids, on functional and morphological indices of dystrophic progression in mdx mice: a pharmacological approach. *Neuropathol. Appl. Neurobiol.* 33:344–59.
5. Porreca E, *et al.* (1999) Haemostatic abnormalities, cardiac involvement and serum tumor necrosis factor levels in X-linked dystrophic patients. *Thromb. Haemost.* 81:543–6.
6. Mourkioti F, Rosenthal N. (2008) NF-kappaB signaling in skeletal muscle: prospects for intervention in muscle diseases. *J. Mol. Med. (Berl.)* 86:747–59.
7. Li H, Lin X. (2008) Positive and negative signaling components involved in TNFalpha-induced NF-kappaB activation. *Cytokine.* 41:1–8.
8. Kumar A, Boriek AM. (2003) Mechanical stress activates the nuclear factor-kappaB pathway in skeletal muscle fibers: a possible role in Duchenne muscular dystrophy. *FASEB J.* 17:386–96.
9. Monici MC, Aguennouz M, Mazzeo A, Messina C, Vita G. (2003) Activation of nuclear factor-kappaB in inflammatory myopathies and Duchenne muscular dystrophy. *Neurology.* 60:993–7.
10. Messina S, *et al.* (2011) Activation of NF-kappaB pathway in Duchenne muscular dystrophy: relation to age. *Acta Myol.* 30:16–23.
11. Cai D, *et al.* (2004) IKKbeta/NF-kappaB activation causes severe muscle wasting in mice. *Cell*. 119:285–98.
12. Kumamoto T, *et al.* (2000) Proteasome expression in the skeletal muscles of patients with muscular dystrophy. *Acta Neuropathol.* 100:595–602.
13. Hasselgren P-O. (2007) Ubiquitination, phosphorylation, and acetylation: triple threat in muscle wasting. *J. Cell. Physiol.* 213:679–89.
14. Rudnicki MA, *et al.* (1993) MyoD or Myf-5 is required for the formation of skeletal muscle. *Cell.* 75:1351–9.
15. Guttridge DC, Mayo MW, Madrid LV, Wang CY, Baldwin AS. (2000) NF-kappaB-induced loss of MyoD messenger RNA: possible role in muscle decay and cachexia. *Science.* 289:2363–6.
16. Hnia, *et al.* (2008) L-arginine decreases inflammation and modulates the nuclear factor-κB/matrix metalloproteinase cascade in mdx muscle fibers. *Am. J. Pathol.* 172:1509–19.
17. Pan Y, *et al.* (2008) Curcumin alleviates dystrophic muscle pathology in mdx mice. *Mol. Cell*s. 25:531–7.
18. Messina S, *et al.* (2011) The soy isoflavone genistein blunts nuclear factor kappa-B, MAPKs and TNF-alpha activation and ameliorates muscle function and morphology in mdx mice. *Neuromuscul. Disord.* 21:579–89.
19. Reay DP, *et al.* (2011) Systemic delivery of NEMO binding domain/IKKgamma inhibitory peptide to young mdx mice improves dystrophic skeletal muscle histopathology. *Neurobiol. Dis.* 43:598–608.
20. Lin S-C, *et al.* (2008) Molecular basis for the unique deubiquitinating activity of the NF-kappaB inhibitor A20. *J. Mol. Biol.* 376:526–40.
21. Wertz IE, *et al.* (2004) De-ubiquitination and ubiquitin ligase domains of A20 downregulate NF-kappaB signalling. *Nature.* 430:694–9.
22. Charan RA, Hanson R, Clemens PR. (2012) Deubiquitinating enzyme A20 negatively regulates NF-κB signaling in skeletal muscle in mdx mice. *FASEB J.* 26:587–95.
23. Inagaki K, *et al.* (2006) Robust systemic transduction with AAV9 vectors in mice: efficient global cardiac gene transfer superior to that of AAV8. *Mol. Ther.* 14:45–53.
24. Wang Z, *et al.* (2005) Adeno-associated virus serotype 8 efficiently delivers genes to muscle and heart. *Nat. Biotechnol.* 23:321–8.
25. Louboutin JP, Wang L, Wilson JM. (2005) Gene transfer into skeletal muscle using novel AAV serotypes. *J. Gene Med.* 7:442–51.
26. Wang B, *et al.* (2008) Construction and analysis of compact muscle-specific promoters for AAV vectors. *Gene Ther.* 15:1489–99.
27. Hayden MS, Ghosh S. (2004) Signaling to NF-kappaB. *Genes Dev.* 18:2195–224.
28. Tisdale MJ. (2005) The ubiquitin-proteasome pathway as a therapeutic target for muscle wasting. *J. Support. Oncol.* 3:209–17.
29. Grounds MD. (1991) Towards understanding skeletal muscle regeneration. *Pathol. Res. Pract.* 187:1–22.
30. Sethi G, Sung B, Aggarwal BB. (2008) Nuclear factor-kappaB activation: from bench to bedside. *Exp. Biol. Med. (Maywood)* 233:21–31.
31. Bakkar N, *et al.* (2008) IKK/NF-kappaB regulates skeletal myogenesis via a signaling switch to inhibit differentiation and promote mitochondrial biogenesis. *J. Cell Biol.* 180:787–802.
32. Deconinck N, Bernard D. (2007) Pathophysiology of duchenne muscular dystrophy: current hypotheses. *Pediatr. Neurol.* 36:1–7.
33. Ervasti JM. (2007) Dystrophin, its interactions with other proteins, and implications for muscular dystrophy. *Biochim. Biophys. Acta.* 1772:108–17.
34. Tang Y, *et al.* (2010) Inhibition of the IKK/NF-kappaB pathway by AAV gene transfer improves muscle regeneration in older mdx mice. *Gene Ther.* 17:1476–83.
35. Glass DJ. (2005) Skeletal muscle hypertrophy and

atrophy signaling pathways. *Int. J. Biochem. Cell Biol.* 37:1974–84.
36. Kandarian SC, Jackman RW. (2006) Intracellular signaling during skeletal muscle atrophy. *Muscle Nerve.* 33:155–65.
37. Spencer MJ, Tidball JG. (2001) Do immune cells promote the pathology of dystrophin-deficient myopathies? *Neuromuscul. Disord.* 11:556–64.
38. Spencer MJ, Montecino-Rodriguez E, Dorshkind K, Tidball JG. (2001) Helper (CD4(+)) and cytotoxic (CD8(+)) T cells promote the pathology of dystrophin-deficient muscle. *Clin. Immunol.* 98:235–43.
39. Mcdouall RM, Dunn MJ, Dubowitz V. (1990) Nature of the mononuclear infiltrate and the mechanism of muscle damage in juvenile dermatomyositis and Duchenne muscular dystrophy. *J. Neurol. Sci.* 99:199–217.
40. Rosenschein U, *et al.* (1987) Human muscle-derived, tissue specific, myocytotoxic T cell lines in dermatomyositis. *Clin. Exp. Immunol.* 67:309–18.
41. Jayandharan GR, *et al.* (2011) Activation of the NF-kappaB pathway by adeno-associated virus (AAV) vectors and its implications in immune response and gene therapy. *Proc. Natl. Acad. Sci. U. S. A.* 108:3743–8.
42. Inagaki K, *et al.* (2006) Robust systemic transduction with AAV9 vectors in mice: efficient global cardiac gene transfer superior to that of AAV8. *Mol. Ther.* 14:45–53.
43. Grimm D, *et al.* (2003) Preclinical in vivo evaluation of pseudotyped adeno-associated virus vectors for liver gene therapy. *Blood.* 102:2412–9.
44. Inagaki K, Piao C, Kotchey NM, Wu X, Nakai H. (2008) Frequency and spectrum of genomic integration of recombinant adeno-associated virus serotype 8 vector in neonatal mouse liver. *J. Virol.* 82:9513–24.
45. Guttridge DC, Albanese C, Reuther JY, Pestell RG, Baldwin AS. (1999) NF-kappaB controls cell growth and differentiation through transcriptional regulation of cyclin D1. *Mol. Cell. Biol.* 19:5785–99.
46. Eghtesad S, Jhunjhunwala S, Little SR, Clemens PR. (2011) Rapamycin ameliorates dystrophic phenotype in mdx mouse skeletal muscle. *Mol. Med.* 17:917–24.